Effects of Unsaturation of C_2 and C_3 Hydrocarbons on the Formation of PAHs and on the Toxicity of Soot Particles

Hamisu Adamu Dandajeh[a,*], Nicos Ladommatos[a], Paul Hellier[a], Aaron Eveleigh[a]

[a]Department of Mechanical Engineering, University College London, Torrington Place, London WC1E 7JE, United Kingdom

Abstract

Engineering systems such as gas turbines and internal combustion engines utilise gaseous fuels which produce toxic substances when they are burnt. Among these substances are solid soot particles and gas phase polycyclic aromatic hydrocarbons (PAHs). The link between soot and PAHs has long been established. Firstly, PAHs assemble themselves into larger structures which are the soot particles themselves. Secondly, they are mostly found, adsorbed on the surfaces of soot particles and form their toxic components. This paper presents the results of both gas-phase and particle-phase PAHs generated from pyrolysis of ethane, ethylene, acetylene, propane and propylene in a homogenous laminar flow reactor. The PAHs studied were the US EPA 16 priority PAHs, but emphasis was given to those PAHs classified as possible carcinogens to humans (Group B2). Pyrolysis of five gaseous fuel molecules was carried out within the temperature range of 1050 - 1350 ^{o}C under oxygen free condition and a fixed fuel concentration of 10,000 ppm on C_1 basis. Soot and gas phase products generated within the reactor were sampled from the exit of the reactor. The PAHs from the samples were then extracted using an accelerated solvent extractor (ASE) and their analysis was carried out using gas chromatography coupled to mass spectrometry (GCMS). The experimental results showed that, depending on the temperature at which a fuel is pyrolysed, its degree of unsaturation plays an important role on the type and concentration of PAHs per unit mass of soot and per unit gas volume. The type of PAH produced and its concentration influenced the overall carcinogenic potential of the gaseous and particulate effluent. It was established that the double bonded C_3 propylene produced the highest amount of soot and particle-phase PAHs per unit mass of soot and per unit volume of gas. Propylene also produced soot particles with

the highest carcinogenicity in the temperature range of 1050 - 1250 ^{o}C and the carcinogenicity decreased with temperature increase. The triple bonded C_2 acetylene produced the highest amount of gas phase PAHs per unit volume of gas when compared with other C_2 and C_3 fuels. It was concluded that increasing the unsaturation of a fuel increases its gas phase PAHs in the case of the C_2 fuels and particle phase PAHs in the case of the C_3 fuels. The total PAH distribution was therefore dominated by the gas phase PAHs in the C_2 fuels and particle phase PAHs in the C_3 fuels.

Keywords: PAHs, unsaturation, pyrolysis, fuels, soot, toxicity

[a,*]Corresponding Author: Hamisu Adamu Dandajeh; hamisu.dandajeh.14@ucl.ac.uk; hadandajeh@abu.edu.ng

1.0 Introduction

Serious health and environmental effects of combustion generated particulates makes it necessary to investigate their formation and toxicity. Polycyclic Aromatic Hydrocarbons (PAHs) have long been considered as one of the major precursors for soot particles, while they also form the main toxic components adsorbed onto the particulates [1]. Most of the carcinogenic, mutagenic and teratogenic PAHs [2],[3] can be present either adsorbed onto the particulates or found as breathable gaseous species in the atmosphere. Human mortality cases associated with airbone particulates bearing adsorbed PAHs have been reported in some cities in the United Kingdom [4] and the United States [5].

In light of the above health reports, a number of toxicological assessments of PAHs have been made over several decades by various global agencies [6],[7],[8]. These agencies evaluated and selected several PAHs on the basis of their carcinogenicities. The selection made by the United States Environmental Protection Agency (US EPA) constituted a list of 16 priority PAHs that are now being consistently listed by researchers worldwide in the PAH analysis of environmental samples.

The PAH benzo(a)pyrene has been confirmed as being the most carcinogenic of the 16 EPA PAHs [9] and, consequently, the most studied [10]. In earlier years, the toxicity of the rest of the 15 EPA PAHs was considered as potent as that of benzo(a)pyrene by the EPA itself [11]. Nisbet and Lagoy [12] subsequently evaluated and modified the new toxic equivalence factors (TEF) for each of the 16 EPA PAHs. The TEF indicates the carcinogenic potential of each of the 16 priority PAH relative to benzo(a)pyrene. Nisbet and Lagoy assigned to benzo(a)pyrene and dibenz[a,h]anthracene a TEF of unity, while benzo(a)anthracene, benzo(b)fluoranthene, benzo(k)fluoranthene and indeno(1,2,3-cd)pyrene were assigned a TEF value of 0.1. The remaining 10 PAHs of the US EPA were either 1000 or 100 times less toxic than the aforementioned six PAHs.

A year after Nisbet and Lagoy's study, chrysene was added to the above list of six PAHs by the US EPA itself [13] in the provisional guidance for quantitative risk assessment (EPA/600/R-93/089) and was accorded a TEF value of 0.01. The above aggregate of seven PAHs were then grouped by the US EPA (1993) as Group B2 ('*possibly carcinogenic to humans'*), while 7 out of the remaining 9 PAHs were grouped as '*unclassifiable as to carcinogenicity'* (Group D). The work reported in this paper aimed at investigating the effect of the degree of unsaturation in C_2 and C_3 single-molecule fuels on the formation of the 16 EPA priority PAHs, while focussing mostly on the formation of the Group B2 PAHs. The EPA PAHs investigated are shown in Table 1, where they are ranked in order of their decreasing toxic equivalence factor (TEF).

PAHs produced by some C_2 and C_3 fuels were investigated previously in flames [14],[15],[16] and tube reactors [17],[18],[19]. Advances have also been made using kinetic modelling [20],[21],[22],[23]. However, the characteristics of PAHs in the gaseous phase and those adsorbed onto particles and the relative toxicity of these PAHs with variation in fuel degree of unsaturation are still not precisely understood. Understanding of the linkage between fuel

79 molecular structures and the amount and toxicity of air bone and particulate borne PAHs is still
80 also incomplete.

81 Furthermore, diesel and gasoline fuels contain a mixture of saturated, unsaturated, branched,
82 and aromatic hydrocarbons [24]. In order to understand and address the influence of fuel
83 molecular structure on the formation and emission of toxic PAH molecules, a homologous
84 series of saturated and unsaturated C_2 and C_3 fuel molecules have been assessed; this could
85 lead to insights that could inform the processing of fuels such that they produce fewer toxic
86 PAH emissions.

87 **Table 1: List of 16 Priority PAHs and their Carcinogenic groups as classified by US EPA (1993)**

Sn	PAHs	PAH Abbreviation	Carcinogenic Group	Toxicity Factor	Molecular Weight(g/mole)	Number of Rings	Formula
1	Benzo(a)pyrene	B[a]P	B2	1.0	252	5	$C_{20}H_{12}$
2	Dibenz[a,h]anthracene	D[ah]A	B2	1.0	278	5	$C_{22}H_{14}$
3	Benzo[a]anthracene	B[a]A	B2	0.1	228	4	$C_{18}H_{12}$
4	Indeno[1,2,3-cd]pyrene	I[123cd]P	B2	0.1	276	6	$C_{22}H_{12}$
5	Benzo[b]fluoranthene	B[b]F	B2	0.1	252	5	$C_{20}H_{12}$
6	Benzo[k]fluoranthene	B[k]F	B2	0.1	252	5	$C_{20}H_{12}$
7	Chrysene	CRY	B2	0.01	228	4	$C_{18}H_{12}$
8	Anthracene	ATR	D	0.01	178	3	$C_{14}H_{10}$
9	Benzo[g,h,i]perylene	B[ghi]P	D	0.01	276	6	$C_{22}H_{12}$
10	Acenaphthylene	ACY	D	0.001	152	3	$C_{12}H_8$
11	Fluorene	FLU	D	0.001	166	3	$C_{13}H_{10}$
12	Fluoranthene	FLT	D	0.001	202	4	$C_{16}H_{10}$
13	Naphthalene	NPH	D	0.001	128	2	$C_{10}H_8$
14	Phenanthrene	PHN	D	0.001	178	3	$C_{14}H_{10}$
15	Acenaphthene	ACN	NA	0.001	154	3	$C_{12}H_{10}$
16	Pyrene	PYR	NA	0.001	202	4	$C_{16}H_{10}$

88 **Group B2 are 'possibly carcinogenic to humans' while Group D are 'unclassifiable as to carcinogenicity' NA –Not available*

89 In this paper, a systematic study of both the gas-phase and particle-phase PAHs generated from
90 the pyrolysis of the fuels in a laminar flow reactor was carried out. The PAHs studied were the
91 US EPA 16 priority PAHs, with special attention given to Group B2 PAHs which are classified
92 as possible carcinogens to humans. Pyrolysis of the gaseous fuel molecules was carried out
93 within the temperature range of 1050 - 1350^{o}C under oxygen free condition and a fixed fuel
94 concentration of 10,000 ppm on C_1 basis. Soot and gas phase products generated within the
95 reactor were sampled from the exit of the reactor. The PAHs from the samples were then

extracted using an accelerated solvent extractor (ASE) and their analysis was carried out using gas chromatography coupled to mass spectrometry (GCMS). The oxygen free pyrolysis conditions in the tube reactor and the range of temperatures chosen resemble to a significant extent the conditions in the core of the fuel spray of a diesel engine where, in the early stages of combustion, there is little oxygen available.

2.0 Experimental Approach

2.1 Gaseous Fuel Molecules Tested

Five, CP grade, single components gaseous fuel molecules, sourced from BOC UK, were tested and their properties are shown in Table 2. They included three C_2 fuel molecules (ethane, ethylene and acetylene) and two C_3 fuels (propane and propylene). The percentage purity of each of the gas molecules was at least 99 %. Ethane is a significant component of natural gas, while propane is a principal component of Liquefied Petroleum Gas (LPG).

Table 2: The five fuel molecules tested with their properties at 1.013 bar and 15 ^oC

Sn	Fuel Molecule	Molecular Structure	C/H	Molecular Mass (g/mole)	Boiling point (^oC)	Density (kg/m^3)
1	Ethane	$H_3C{-}CH_3$	0.33	30.07	-88.6	1.28
2	Ethylene	$H_2C{=}CH_2$	0.5	28.05	-103.7	1.19
3	Acetylene	$HC{\equiv}CH$	1	26.04	-84.7	1.11
4	Propane	$H_3C{-}CH_2{-}CH_3$	0.375	44.10	-42.1	1.90
5	Propylene	$H_3C{-}CH{=}CH_2$	0.5	42.08	-47.6	1.81

The purpose of this paper is to investigate the following aspects of the influence of unsaturation of C_2 and C_3 Fuels on PAH formation:

i) Confirm the influence of the degree of unsaturation on the propensity of a fuel to form soot in the tube reactor used for this study

ii) Study the influence of fuel unsaturation on the condensation of PAHs on soot particles and the production of PAHs as gas phase species

iii) Study the influence of fuel unsaturation on the toxicity of the Group B2 PAHs found on soot particles under pyrolysis conditions

iv) Consider mechanisms that lead to the formation of gas and particle phase PAHs, and in particular, those mechanisms that lead to the formation of Group B2 PAHs

2.2 Sample Generation

Soot and gaseous samples were generated by means of pyrolysis using a tube reactor at temperatures ranging from 1050 -1350 °C. Figure 1 shows a schematic of the experimental set-up. The experimental facility consisted of a reactor temperature control system, oxygen-free nitrogen and fuel gas supplies, mass flow controllers (MFC) (1) for nitrogen and the gaseous fuel, a nitrogen heater, fuel inlet (2), nitrogen/fuel, static mixer (3), circulating cooling water (4), insulated heated nitrogen/fuel lines, tube heater (5), DMS 500 particle size spectrometer instrument and its dilution cyclone, DMS 500 sampling probe (6), soot sampling probe (7), particulate filter housing, a stainless steel resin (XAD-2) cartridge holder, gas volumetric meter, vacuum pump, and a PC for system control and storing data.

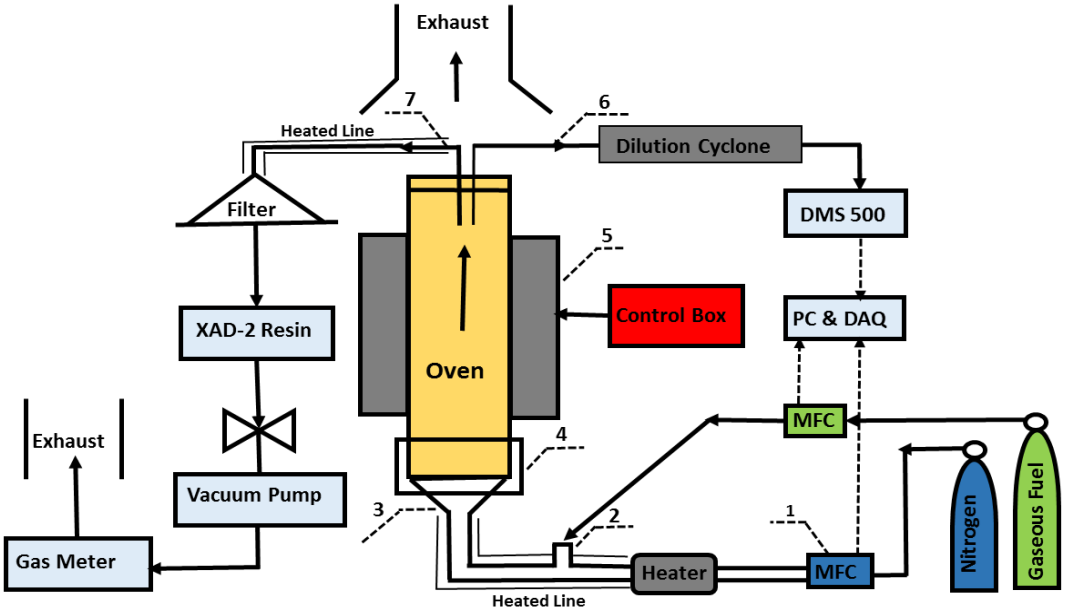

Fig.1: Schematics of the experimental set-up: 1) mass flow controller (MFC) 2) fuel inlet 3) static mixer 4) circulating cooling water 5) tube furnace 6) DMS 500 sampling probe 7) soot sampling probe

The carrier gas used during the pyrolysis of all the gaseous fuel molecules was nitrogen and was metered at a constant flow rate of 20 L/min (at STP conditions) using a MFC (1). All five fuel molecules were supplied to the pyrolyser at a fixed carbon flow rate of 10,000 ppm on C_1 basis. Thus, for example, the volumetric flow rate of ethane was approximately one and half times as high (ml/min) as that of propane. The flow rate of each fuel molecule is shown in Table 3. Ethane was also used as the baseline fuel for daily repeat checks and for drift in the reactor systems and associated instrumentation. The fuel molecules were injected into the nitrogen stream via software-controlled solenoid valves.

Table 3: The concentrations of five fuel molecules tested (ppm is on molar basis)

Sn	Fuel Molecule	Fuel Flow rate (mL/min)	Fuel Flow rate on C_1 basis (ppm)
1	Ethane	99.80	10,000
2	Ethylene	99.95	10,000
3	Acetylene	98.90	10,000
4	Propane	69.90	10,000
5	Propylene	64.80	10,000

An electrical tape heater surrounded and heated the nitrogen line connected to the fuel inlet (2). A proportional integral derivative (PID) controller maintained the nitrogen gas temperature at 150 °C. In order to avoid condensation of gas phase PAHs, the soot sampling stainless steel probe (7) that led to the filter housing was heated by a tape heater and controlled at a temperature of 120 °C by a separate PID controller.

Immediately when fuel was introduced into the nitrogen stream, the combined fuel and nitrogen stream passed through a static mixer (3). The mixer was packed with 8mm stainless steel ball bearings which were located at the tube reactor inlet. The mixer ensured that the combined streams were homogeneously mixed. The temperature in the mixer was maintained at >180 °C with the aid of a type K thermocouple. The tube reactor was 1440 mm long and had 104 mm diameter. The alumina tube was vertically positioned in an electric furnace and about 600 mm of the tube central length was heated, and was found to be uniform. The tube heated section

156 was maintained by an electrical PID controlled system at temperatures within the range of
157 1050 – 1350 °C. The longitudinal temperature profile of the reactor used in this work has been
158 recorded previously [25]. The profile is typical of such tube reactors as reported in Glarborg et
159 al. [26]. The gas residence time (t_r) can be calculated using equation 1.

160 $$t_r(s) = \frac{V_r(L)}{Q(L/s)} \quad (1)$$

161 Where V_r is the volume of the 600mm reaction zone of the reactor, and Q is the volumetric
162 flow rate at the reaction temperatures tested. The residence time was therefore dependent on
163 the reactor temperature (T), and can be expressed as 4470/T (s).
164
165 Soot particles generated within the reactor were sampled by means of a stainless steel probe
166 connected to a vacuum pump. The probe was placed at the outlet of the reactor using a
167 12.5 mm stainless steel tube (7). The flow rate of the vacuum pump was maintained at
168 < 18 L/min using a control valve. Between the soot sampling probe and the vacuum pump, a
169 particulate filter and a resin based system were placed to collect particulate and gaseous PAHs
170 respectively. The soot samples were collected on a glass micro fibre filter (70 mm diameter,
171 0.7 µm pore size, 75 g/m^2 mass, 310 s filtration speed) (Fisher Scientific UK). A glass fibre
172 filter was chosen due to its PAH-inertness and heat resistance properties, and was also found
173 suitable by many other studies [27], [17],[18]. The mass of the filter was measured before and
174 after sampling on a high precision mass balance (d = ± 0.001 mg) in order to obtain the soot
175 mass collected. The filter was first baked in an oven, to a temperature of 120 ^{o}C for 8 hours so
176 as to minimize the moisture in the filter and used immediately upon being removed from the
177 oven. The filter holder was also maintained at a temperature of 120 ^{o}C. Repeatability tests with
178 ethane as the baseline fuel was conducted at 4 different test days. The repeat results for mass
179 concentration from ethane pyrolysis showed that the measurement process was repeatable
180 (Table 4), to satisfactory levels, with the standard deviations in soot masses generated from

ethane pyrolysis being 1mg (20 %) at the temperature of 1050 ^{o}C and 14 mg (9 %) at the temperature of 1250 ^{o}C.

The gas phase PAHs were trapped onto a Supelco brand Amberlite XAD-2 resin (~0.65 mL/g pore volume, 90 Å mean pore size, ~300 m^2/g surface area and density of 1.02 g/mL at 25 °C) (Sigma Aldrich, UK). XAD-2 resin was selected since it was reported by EPA 1999 [27] to have higher collection and retention efficiencies compared to other sampling materials such as Tenax® and polyurethane foam (PUF). A preliminary PAH analysis carried out with both the resin and PUF confirmed that the resin was more suitable for trapping gaseous PAHs. A glass cartridge was first loaded with 5g of the XAD-2 resin sandwiched between two pieces of glass wool. The cartridge was then inserted into a custom-made stainless steel housing. The resin housing was connected in series after the particulate filter. The gas volume passed through both the filter and the XAD-2 resin was measured by a diaphragm volumetric gas meter (Q_{max} = 6 m^3/h) sourced from Bell flow Systems UK. During ethylene pyrolysis at 1150 °C for example, the DMS 500 instrument (particle spectrometer), was used to assess the sample in the flow before and after the filter housing. It was found that particles up to 200 nm were sampled before the filter. After the filter, no particle > 10 nm was passed onto the XAD-2 resin. Therefore, only clean gases without particles > 10 nm entered the XAD-2 resin holder. Particles < 10 nm recorded by the DMS 500 were considered to be condensed species.

The sampling durations for soot and gaseous PAHs was 15 min at all temperatures tested. This duration was chosen after an optimisation exercise in order to trap sufficient mass of soot for subsequent GCMS analysis. The mass of soot and volume of gas passed through the particulate filter and the XAD-2 resin for each test duration were measured. The filter gravimetric soot mass measurements and calculated soot mass concentrations at each temperature, for the C_2 and C_3 fuels are shown in Table 4. The particulate and the gas phase samples collected were

stored separately in 90 mm diameter plastic petri dishes and wrapped with para-film tape and immediately frozen and stored in dark frozen conditions before further analysis.

2.3 Sample Extraction

The extraction of PAH species from the soot and resin samples was carried out using an Accelerated Solvent Extractor (ASE) (Thermo Scientific Dionex-150). ASE is an automated technique for rapidly extracting molecules such as PAHs at elevated temperature and pressure. It is a recommended technique by the EPA (Method 3545, SW-846, draft update IVA) for extracting PAHs [28]. ASE has advantage over classical Soxhlet extraction, including large solvent reduction, faster extraction times by up to an order of magnitude and improved extraction efficiency and recovery [29]. All samples were extracted using dichloromethane (DCM) solvent. DCM was used as a solvent because it has boiling point far lower than that of all the 16 PAHs of interest and has long been used [30] for PAH recoveries. The extraction was carried out using a 10 mL solvent/sample cell at a temperature of 125 ^{o}C and pressure of 100 bar (one static cycle at 5 min, purge time of 60 s, 40 % rinse volume, extraction time of 15min and total extracted volume 20 mL per single extraction) [29]. Extraction of PAHs from each particulate and resin sample was repeated three times in the same collection vial in order to ensure that all the extractable PAHs were extracted. The first, second and third extractions accumulate the total extraction volume to 60 mL per sample. The efficiency of the extraction method was evaluated using 84.6 mg of ethylene soot generated from the reactor at 1150 ^{o}C and was found to be 90 %. PAH recoveries of each of the 16 PAHs were calculated relative to the conventional atmospheric Soxhlet extraction and were found to be in the range of 82 – 120 %. Several authors [30], [31] had also compared the recovery efficiencies of ASE and conventional Soxhlet and their results were similar to those reported in this study. In order to prevent any deterioration of PAHs during deep-freeze storage, all the samples were extracted within one week of their generation.

2.4 Sample Concentration

Most of the DCM in the 60 mL extracted volume was evaporated by bubbling gently a nitrogen stream at 5 L/min through the extraction vial containing the extracts. The extraction vial was situated in a custom-made stainless steel PID controlled heating mantle. Each extract was initially concentrated from 60 mL down to about 15 mL and was then transferred into a graduated glass tube (0 to 15 m L) (VWR UK). The 15 mL extract was then concentrated further, down to 1 mL.

2.5 Sample Analysis

The concentrated 1 mL extracts were analysed with gas chromatography coupled to mass spectrometry (GCMS) (Agilent 7890B GC coupled with 5977A MSD to HP-5 column of: 30 m x 250 µm x 0.25 µm). Helium was used as the carrier gas at a flow rate of 1.2 L/min. An automatic liquid sampler (ALS) was used, injecting 1 µL of each sample in a split-less mode. The GC oven was heated starting with an initial temperature of 50 °C, held for 1 min, followed by a ramp rate of 25 °C/min to 150 °C, held for 1 min. Further ramping of 25 °C/min, increased the temperature to 200 °C, and held for 1 min. Another ramp rate of 3 °C/min, increased the temperature to 230 °C, held for 1 min. Finally, a ramp rate of 8 °C/min increased the temperature to 310 °C, held for 3 min. The total run time of each sample was 33 min. The transfer line temperature was 290 °C. The MS used was single quadrupole in electron ionization (EI) mode. MS Source temperature was 230 °C and MS quad temperature was 150 °C.

In order to quantify the PAHs in a sample, the GC was first calibrated using a standard QTM PAH Mix certified reference material of initial concentration of 2000 µg/mL in dichloromethane. The standard (Sigma Aldrich, UK) contained the 16 PAH compounds shown in Table 1. Each PAH had certified purity ranging from 98.2 - 99.7 %. The PAH standard was first diluted in DCM in the ratio of 1:50 and then serially diluted further into five calibration

levels in the ratio of 1:5. An internal standard mixture (Sigma Aldrich UK) of concentration equivalent to the middle calibration level (1 μg/mL) was added to each calibration vial based on EPA Method To-13A analysis guidelines for PAHs [27]. The internal standard mixture contained the following 6 compounds and their target PAHs, namely: 1,4-Dichlorobenzene-d4, Naphthalene-d8 (NPH), Acenaphthene-d10 (ACN, ACY, FLR), Phenanthrene-d10 (PHN, ATR, FLT), Chrysene-d12 (PYR, B(a)A, CRY) and Perylene-d12 (B(b)F, B(k)F, B(a)P, I(123cd)P, D(ah)A, B(ghi)P). The GC calibration was carried out by running the five calibration levels. Calibration curves were developed for each of the 16 PAH compounds and their R^2 values were ≥ 98 %. Unknown target PAHs were quantified in a selected ion monitoring (SIM) mode. This was carried out by identifying the target PAHs based on detection of the ions in each PAH molecule and subsequent comparison of the retention times of the ions with those of the QTM PAH Mix calibration standards.

3.0 Results and Discussion

3.1 Effect of unsaturation on Soot Mass

Measured soot mass and calculated soot mass concentrations during the pyrolysis of all the C_2 and C_3 fuels are shown in Table 4. The results from Table 4 showed that, for all the fuels examined, increase in temperature of the reactor from 1050 – 1250 ^oC resulted in increase in the mass concentration of soot collected. This trend was consistent with those reported in the literature [18], [32], [33].

It can be observed from Table 4 that the single bonded ethane and the doubled bonded ethylene produced roughly similar soot mass concentrations, indicating that under the experimental conditions tested, the presence of double bond was not significant in determining the rate of soot formation. In an oxygen/fuel environment [34], one would expect ethylene to soot substantially more than ethane, probably because of increased tendency for ethylene to become acetylene by means of hydrogen abstraction due to oxygen radicals. The absence of oxygen in

280 the pyrolysis reported here does not promote the hydrogen abstraction by means of oxygen
281 radicals.

282 It is also apparent from Table 4 that when the triple bonded acetylene was pyrolysed, the soot
283 formation, in comparison to the other two C_2 fuels, increased considerably. For instance, the
284 soot concentrations generated in acetylene pyrolysis at the temperatures of 1050 ^{o}C and
285 1150 ^{o}C were, respectively, 5 and 2 times those for ethylene. The above observations are
286 supported by the results of other investigations. For example, Ruiz et al. [32] carried out
287 pyrolysis of ethylene and acetylene within the temperature range of 1000 – 1200 ^{o}C in a similar
288 tube reactor and they found that the amount of soot generated from acetylene was higher than
289 that from ethylene at all temperatures.

290 The enhanced soot propensity of acetylene could be that it is directly implicated as a reactive
291 species in the HACA (hydrogen abstraction, acetylene addition) mechanism, which contributes
292 to PAH and particle growth [35]. Mechanistic studies have highlighted the significance of the
293 HACA mechanism in fuel rich hydrocarbon flames [36] and under pyrolysis conditions [19].
294 Acetylene has also been identified as directly involved in the formation of the first aromatic
295 ring [1], this sets it apart from ethane and ethylene, which must both undergo dehydrogenation
296 in order to form acetylene. The large differences in the soot concentrations for ethane, ethylene
297 and acetylene, observed at low temperature in Table 4, reduced significantly at the higher
298 temperatures. Similarly, it can be seen from Table 4 that propylene yielded more soot
299 concentrations than propane at all conditions tested. This is not surprising since propylene
300 (C_3H_6) is a doubled bonded unsaturated C_3 fuel that can produce propargyl radical (C_3H_3)
301 during pyrolysis [37]. Propargyl radicals are also known to be highly instrumental in the
302 formation of the first aromatic ring [38], thus speeding up subsequent PAH growth and initial
303 soot particle inception. This is probably why propylene was more prolific in soot formation.

Higher soot propensity for propylene, when compared with propane, was also reported for flames by Wang and Chung [39].

Table 4: soot mass and soot concentrations from filter gravimetric measurements

Temperature (°C)	Ethane		Ethylene		Acetylene	
	Soot Mass (mg)	Soot Conc. (mg/m^3)	Soot Mass (mg)	Soot Conc. (mg/m^3)	Soot Mass (mg)	Soot Conc. (mg/m^3)
1050	5.100±1.000	16.00	8.000	25.70	36.30	119.0
1150	75.00±11.00	433.5	84.60	485.5	142.4	863.0
1250	153.0±14.00	956.3	155.4	953.4	202.6	1282
1350	124.5±11.00	793.0	135.0	849.1	169.3	1092

Temperature (°C)	Propane		Propylene	
	Soot Mass (mg)	Soot Conc. (mg/m^3)	Soot mass (mg)	Soot Conc. (mg/m^3)
1050	31.40	88.20	45.90	173.2
1150	146.3	774.1	202.0	1080
1250	202.9	1222	221.4	1366
1350	157.5	966.3	222.6	1436

***Conc. is equivalent to concentration*

Finally, looking at all the results for the C_2 and C_3 fuels in Table 4, it can be concluded that the tendency of a fuel molecule to soot increases when its unsaturation level increases within the homologous series of the fuels shown in the Table, however, this does not seem to apply in the case of ethane and ethylene.

3.2 Gas and Particle phase PAH Distributions

Fig.2 shows the PAH results for ethane. The figure shows the PAHs extracted from the XAD-2 resin and from the particulate collected on the filter. In Fig.2, the results of the PAHs extracted from the resin are labelled "GP" (gas phase) PAHs while those extracted from particulate are labelled "PP" (particle phase) PAHs. The error bars in Fig.2 denote standard deviations. Fig.2a shows the gas phase PAH mass normalised with the volume of gas passed through the resin and the filter (in series) (i.e., gas phase PAH concentration), while Fig.2b shows the corresponding concentration of the mass of PAH extracted from the particulate per unit volume of gas passed through the filter. Fig. 2c shows the mass of PAH extracted from the particulate normalised with the particulate mass. Finally, Fig.2d shows the total PAH (gas and particulate borne) normalised by the volume of gas.

It can be observed from Fig.2a that smaller PAHs ranging from naphthalene (MW= 128 g/mole) to pyrene (MW= 202 g/mole) were consistently identified in the gas phase (GP) in significantly high concentrations at all the temperatures tested. This trend was consistent with those reported in the literature[17],[18]. The GP PAHs have higher vapour pressures and lower boiling points which reduces their condensation and adsorption rates onto the particulates. The GP PAH concentration (Fig.2a) decreased with temperature rise from 1050 - 1350 ^{o}C. One possible explanation for this decrease in the concentrations of GP PAH with temperature rise was that, at a temperature of 1050 ^{o}C for example, the kinetics for their growth into larger PAH was slower, hence, they continuously accumulate in the gas phase in relatively high concentrations. At higher temperatures, it is expected that the rate of growth of a specific PAH into larger PAH accelerated, exceeding the rate at which the specific PAH was formed from smaller PAHs. In this way, one would expect the concentration of a specific PAH to be dependent on the balance between its formation through smaller PAHs and its change into larger PAHs through growth. As PAHs grew to larger structures, these were incorporated into new or the nascent soot particles.

Figure 2a shows that at a temperature of 1050 ^{o}C heavier PAHs (CRY, B(k)F, I(123cd)P and B(ghi)P) occur in both GP and PP, but at about 1150 ^{o}C and above, they are predominantly found in the PP. This could be due to surface area available for PAH condensation at lower temperatures. The disappearance of these four PAHs from the GP at higher temperatures (>1150 ^{o}C) could therefore, be due to the increased rate of soot and particle surface area available for PAH condensation and adsorption. Fig.2b shows that five lighter PAHs (NPH, ACY, FLR, PHN and FLT – see Table 1 for PAH abbreviations) were found in the particle phase (PP) and these were at low concentrations. Also, heavier PAHs ranging from PYR to B(ghi)P (MW = 276 g/mole) were found in the particle phase (PP) at high concentrations.

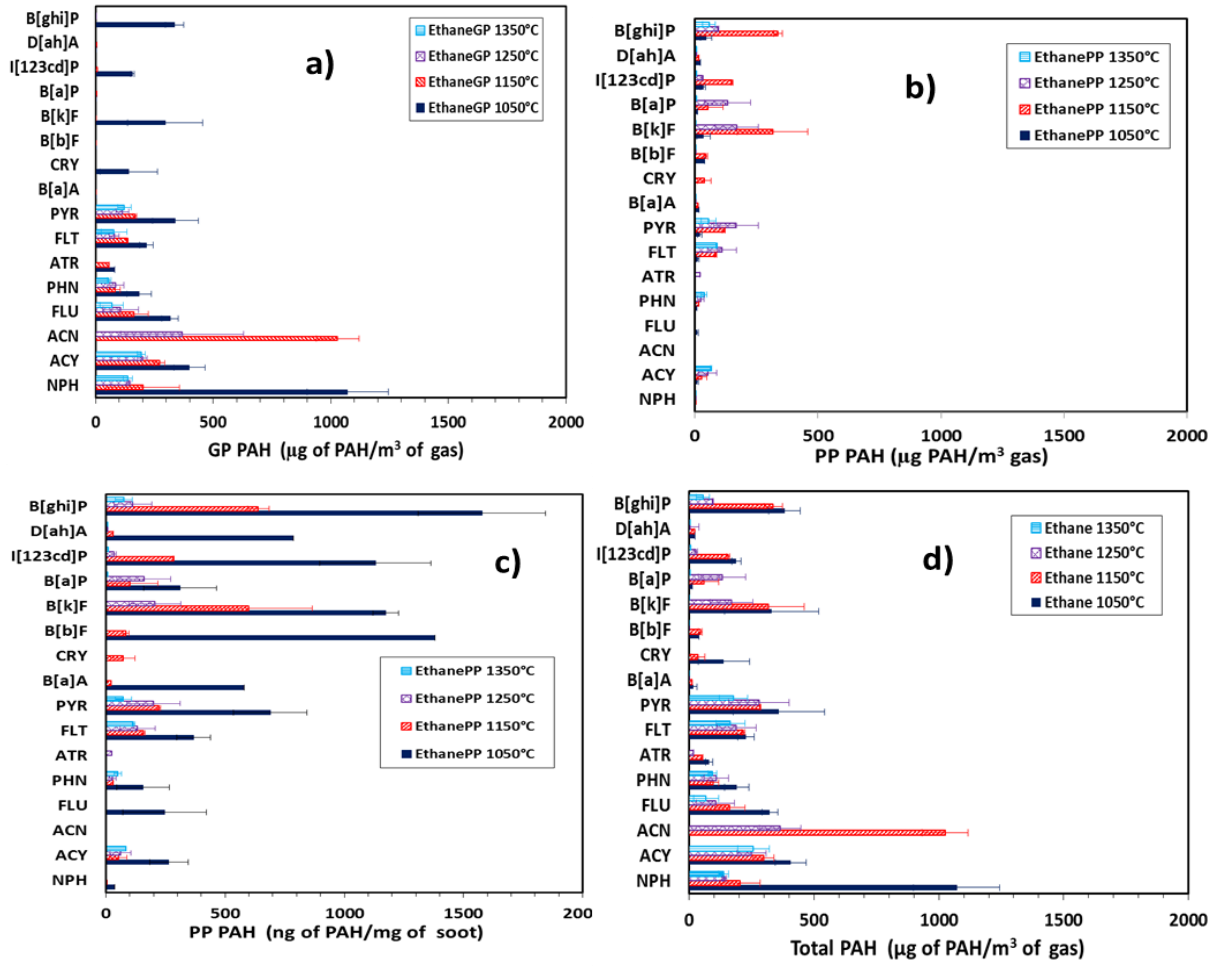

Fig. 2: The distributions of PAHs during ethane pyrolysis from temperature range of 1050 - 1350°C: a) Gas Phase (GP) (µg of PAH/m^3 of gas) b) Particle Phase (PP) (µg of PAH/m^3 of gas) c) Particle Phase (ng of PAH/mg Soot). d) Total PAHs (GP +PP) (µg of PAH/m^3 of gas). Error bars denote the standard deviation.

The PP PAHs normalised with the mass of soot from which they were extracted is shown in Fig.2c, it can be observed that both the lighter and heavier PAHs on the soot particles decreased with temperature rise. For example, the concentrations of B(g,h,i)P per unit mass of soot at a temperature of 1050 °C decreased by 2.5 times at 1150 °C, 14 times at 1250 °C and 21 times at 1350 °C. This is believed to be related to a decrease, with rising temperature, in the number of soot particles size caused by agglomeration of primary soot particles which led to the corresponding increase in the sizes of the soot particles sampled. Hence, the surface area available for the PP PAHs to condense onto decreased. Another explanation to decrease in the PAH mass on the soot particle is that temperature increase led to more carbon being converted

360 to soot, hence, less carbon was available as PAHs. It is also possible that the decrease in the
361 amount of PP PAHs at higher temperature was due to more organised soot particle micro-
362 structure [33] which made them less reactive [32] and thus, they might have therefore
363 accommodated smaller amounts of PAHs.

364 Fig.2d combines the GP and PP PAHs; the total PAHs per unit volume of gas is shown in the
365 figure, which was drawn by adding the GP PAHs in Fig.2a to the PP PAHs in Fig.2b. The total
366 PAH distribution includes most of the 16 EPA priority PAHs. It can be observed from Fig.2d
367 that the trend in the concentrations of the total PAHs resembled more that of the GP than that
368 for the PP PAHs. Thus, the total PAH found in the gaseous and particulate phases in ethane
369 pyrolysis was dominated by the GP PAHs. The variations of GP and PP PAHs per unit volume
370 of gas, and of the PP per unit mass of soot for ethane pyrolysis was broadly similar with those
371 found for the other C_2 fuels and all the C_3 fuels tested. Tables 5, 6 and 7 summarise the
372 variations of the GP and PP PAHs for all the fuels tested. Among all the PAH results displayed
373 in those Tables, only ethane results are shown in Figure 2 as an example, and also as a guide
374 for discussion.

375 The relative contributions of the GP and PP PAHs to the total PAH are shown in Fig.3 for the
376 C_2 and C_3 fuels investigated. It can be seen from Fig.3a that at the temperature of 1050 ^oC, for
377 example, the proportion GP from ethane pyrolysis was 95 %. This proportion decreased to
378 64 % and 58 % at 1150 ^oC and 1250 ^oC, respectively. In the case of ethylene (Fig.3b), the
379 proportion of GP dropped gradually from 93 % to 66 % when the temperature was raised from
380 1050 – 1350 ^oC. However, Fig.3c shows that the pattern for acetylene pyrolysis was largely
381 dominated by the GP PAHs in the temperature range of 1050 – 1250 ^oC by a constant
382 proportion of approximately 84 %, followed by a marked drop of this proportion to 50 % at
383 1350 ^oC.

384 **Table 5: Normalised Gas and Particle Phase PAHs of the remaining C_2 Fuels (µg of PAH/m^3 of gas) (*_bdl denotes 'below detection limit' of the PAH_)**

	Ethane								Ethylene								Acetylene PAHs							
	1050 ºC		1150 ºC		1250 ºC		1350 ºC		1050ºC		1150ºC		1250 ºC		1350 ºC		1050ºC		1150ºC		1250ºC		1350ºC	
PAHs	**GP**	**PP**	**GP**	**PP**	**GP**	**PP**	**GP**	**PP**	**GP**	**PP**	**GP**	**PP**	**GP**	**PP**	**GP**	**PP**	**GP**	**PP**	**GP**	**PP**	**GP**	**PP**	**GP**	**PP**
NPH	1071	1.04	201.7	2.139	141.5	1.77	137	1.84	300	1.24	212	2.7	246	2.2	215	2.08	1337	1.62	1280	2.7	685	2.09	279	2.31
ACY	399.6	7.73	272.0	27.51	199.5	51.3	194	64.2	315	bdl	258	bdl	276	bdl	229	9.84	407.8	bdl	341	41	352	14.5	160	bdl
ACN	bdl	bdl	1030	bdl	368.1	bdl	bdl	bdl	853	bdl	698	bdl	473	bdl	bdl	bdl	530.6	bdl	627	bdl	412	bdl	bdl	bdl
FLU	316.7	7.22	163.9	bdl	106.7	bdl	69.6	bdl	176	bdl	162	bdl	120	bdl	bdl	bdl	190.9	bdl	206	bdl	99.6	bdl	86.6	bdl
PHN	186.5	4.54	81.69	15.28	85.97	23.2	57.2	37.3	71.0	1.59	69	3.47	73.9	2.82	68.3	2.67	77.04	2.09	70.6	3.4	72.6	10.7	44.7	32.7
ATR	bdl	bdl	bdl	bdl	bdl	bdl	bdl	bdl	281	bdl	219	bdl	bdl	101	bdl	83.2	574.9	bdl	bdl	bdl	bdl	bdl	bdl	190
FLT	216.8	10.7	135.1	83.11	79.1	111	78.8	87.8	165	11.2	123	57.8	164	34.0	135	56.9	173.2	24.7	167	47	111	46.3	61.2	110
PYR	339.8	20.2	167.4	117.9	114.1	166	122	55.5	283	23.1	174	102	153	67.6	150	67.5	335.3	58.9	295	86	215	82.7	56.9	212
B[a]A	0.204	0.25	0.448	0.517	0.427	0.43	0.48	0.443	0.24	0.30	0.4	0.65	0.49	0.53	0.54	0.5	0.283	0.39	0.56	0.6	0.51	0.51	0.60	0.56
CRY	140.9	bdl	bdl	37.91	bdl	bdl	bdl	bdl	34.7	bdl	bdl	bdl	bdl	bdl	bdl	16.3	74.89	27.3	bdl	bdl	bdl	bdl	bdl	bdl
B[b]F	0.718	0.88	1.578	1.82	1.503	1.5	1.70	1.56	0.82	1.05	1.5	2.3	1.72	1.87	1.91	1.77	0.998	33.8	1.98	2.3	1.79	1.78	2.11	1.96
B[k]F	296.1	34.3	2.08	315.2	1.982	170	2.25	2.06	138	40.9	2.0	235	2.27	2.46	2.53	2.33	174.3	104	2.62	88	2.35	55.9	2.78	2.59
B[a]P	2.422	9.09	5.32	53.45	5.07	133	5.75	5.30	63.4	9.45	5.0	55.1	5.82	6.3	6.46	5.96	95.14	97.3	6.71	175	6.00	44.1	7.13	35.4
I[123cd]P	157.3	33.1	7.43	149.5	7.075	28	8.02	7.35	3.90	29.6	7.1	217	8.12	27.3	9.01	15.6	26.58	143	9.35	47	8.37	17.9	9.96	9.25
D[ah]A	2.736	3.37	6.01	6.936	5.727	5.73	6.49	5.95	3.20	4.02	5.7	8.77	6.57	7.12	7.30	6.74	3.803	5.26	7.57	8.7	6.78	6.78	8.06	7.48
B[ghi]P	336.7	46.1	bdl	337.3	2.423	93.5	2.75	57.0	205	70.8	2.4	367	2.78	271	3.09	162	35.25	261	3.23	219	2.87	137	3.41	3.17

385

386 **Table 6: Normalised Particle Phase PAHs of C_2 and C_3 Fuels (x 10 ng of PAH/mg of soot) (*_bdl denotes 'below detection limit' of the PAH_)**

	1050 ºC					1150 ºC					1250 ºC					1350 ºC				
PAHs	**C_2H_6**	**C_2H_4**	**C_2H_2**	**C_3H_8**	**C_3H_6**	**C_2H_6**	**C_2H_4**	**C_2H_2**	**C_3H_8**	**C_3H_6**	**C_2H_6**	**C_2H_4**	**C_2H_2**	**C_3H_8**	**C_3H_6**	**C_2H_6**	**C_2H_4**	**C_2H_2**	**C_3H_8**	**C_3H_6**
NPH	3.56	4.3	1.37	2.6	1.79	0.41	0.62	0.3	0.28	0.23	0.22	0.23	0.18	0.14	0.2	0.24	0.27	0.14	0.21	0.14
ACY	26.4	bdl	bdl	bdl	87.8	5.21	bdl	4.8	7.3	11.8	6.15	Bdl	1.23	1.93	2.9	8.5	1.26	bdl	6.61	4.84
ACN	bdl	bdl	bdl	bdl	bdl	bdl	bdl	bdl	bdl	bdl	bdl	bdl	bdl	bdl	bdl	bdl	bdl	bdl	bdl	bdl
FLU	24.7	bdl	bdl	bdl	bdl	bdl	bdl	bdl	bdl	bdl	bdl	bdl	bdl	bdl	bdl	bdl	bdl	bdl	bdl	bdl
PHN	15.5	5.5	1.75	3.4	43	2.9	0.8	0.39	2.53	3.9	2.78	0.3	0.91	1.92	2.2	4.9	0.34	1.94	3.68	3.31
ATR	bdl	bdl	bdl	bdl	332	bdl	bdl	bdl	bdl	bdl	bdl	10.8	bdl	13.3	2.8	bdl	10.6	11.2	50.5	2.24
FLT	36.7	38.7	20.7	39	64.6	15.7	13.3	5.5	8.78	10.6	13.3	3.62	3.91	7.93	5.8	11.6	7.26	6.5	10.5	5.77
PYR	69.0	79.8	49	83	109	22.3	23.5	10	14.5	16.7	19.9	7.2	6.99	12	20	7.3	8.62	12.5	8.25	15.0
B[a]A	0.86	1.03	0.33	0.6	0.41	0.1	0.15	0.07	0.07	0.06	0.05	0.06	0.04	0.03	0.04	0.06	0.06	0.03	0.05	0.03
CRY	bdl	bdl	23	27	78.9	7.18	bdl	bdl	bdl	6.5	bdl	bdl	bdl	bdl	bdl	bdl	2.08	bdl	bdl	bdl
B[b]F	3.02	3.64	28	2.2	1.43	0.35	0.53	0.26	0.24	0.2	0.18	0.20	0.15	0.12	0.13	0.21	0.23	0.12	0.18	0.12
B[k]F	117	141	87	239	306	59.7	54.1	10.2	50	55.2	20.4	0.26	4.73	8.82	3.7	0.27	0.30	0.15	0.24	0.15
B[a]P	31.1	32.7	82	154	121	10.1	12.7	20.2	7.42	16.9	15.9	0.67	3.73	9.85	3.5	0.70	0.76	2.09	0.61	0.39
I[123cd]P	113	106	120	241	104	28.3	50.1	5.44	22	28.3	3.36	2.91	1.51	1.61	0.6	0.97	2.0	0.55	0.84	0.55
D[ah]A	11.5	1.39	4.42	109	52	1.31	2.02	0.1	0.91	0.75	0.69	0.76	0.57	0.44	0.48	0.79	0.86	0.44	0.68	0.44
B[ghi]P	158	245	220	238	244	6.39	84.7	25.3	33.4	40.6	11.2	28.9	11.6	13	5.04	7.53	20.7	0.19	0.29	0.19

387

388 **Table 7: Normalised Gas and Particle Phase PAHs of C3 Fuels (µg of PAH/m^3 of gas)**

		Propane PAHs								Propylene PAHs							
		1050 °C		1150 °C		1250 °C		1350°C		1050°C		1150 °C		1250 °C		1350°C	
Sn	**PAHs**	**GP**	**PP**	**GP**	**PP**	**GP**	**PP**	**GP**	**PP**	**GP**	**PP**	**GP**	**PP**	**GP**	**PP**	**GP**	**PP**
1	NPH	207	2.31	195	2.19	131	1.68	121	2.03	426	2.91	198	2.50	146	2.04	94	1.95
2	ACY	346	bdl	266	56.6	241	23.6	162	63.9	275	152	263	127	166	39.5	138	69.4
3	ACN	326	bdl	bdl	bdl	bdl	bdl	bdl	bdl	791	bdl	653	bdl	bdl	bdl	bdl	bdl
4	FLU	193	bdl	138	bdl	69.8	bdl	bdl	bdl	238	bdl	197	bdl	93.5	bdl	bdl	bdl
5	PHN	71.7	2.97	46	19.6	32.3	23.4	24	35.6	73.8	74.5	52	42.5	2.18	29.9	29	33.1
6	ANT	bdl	bdl	bdl	bdl	331	163	bdl	487	bdl	576	bdl	bdl	bdl	384	bdl	322
7	FLR	172	34.1	120	67.9	69.5	96.9	58.5	101	149	112	114	114	58.9	79.3	26	82.6
8	PYR	360	72.9	155	112	96.7	147	90.1	79.7	208	188	156	180	39.3	274	26	215
9	B[a]A	0.22	0.56	0.4	0.53	0.52	0.40	0.45	0.48	0.33	0.71	0.5	0.60	0.41	0.49	0.5	0.47
10	CRY	bdl	24.0	bdl	29.4	bdl	bdl	bdl	bdl	53.8	137	bdl	69.9	bdl	bdl	bdl	bdl
11	B[b]F	0.78	1.97	1.5	1.85	1.83	1.41	1.58	1.72	1.15	2.47	1.6	2.13	1.44	1.73	1.8	1.66
12	B[k]F	260	211	1.9	387	2.42	108	2.08	2.27	148	531	2.1	597	1.91	50.0	2.4	2.19
13	B[a]P	60.6	136	5.1	57.5	6.19	120	5.33	5.82	34.5	209	5.5	183	4.88	47.6	6.1	5.6
14	I[123cd]P	57.3	213	7.0	171	8.63	19.6	7.44	8.12	5.41	181	7.7	306	6.81	8.17	8.6	7.82
15	D[ah]A	3.08	95.9	5.7	7.08	6.99	5.37	6.02	6.57	4.38	90.1	6.2	8.11	5.51	6.61	6.9	6.33
16	B[ghi]P	101	210	2.4	258	2.95	159	2.54	2.78	1.85	422	2.6	438	2.33	68.9	2.9	2.67

389 **bdl is below detection limit*

390 The decrease in the proportion of GP PAHs due to temperature increase seen in Fig.3,a,b & c
391 could generally be linked with a corresponding increase in the mass of soot generated and to
392 increasing PP PAHs condensed on the soot particles. For example, in the case of ethylene
393 pyrolysis, the soot mass concentration sampled at 1050 °C was 25.7 mg/m^3 and it increased
394 remarkably by a factor of 19 and 37 at temperatures of 1150 °C and 1250 °C respectively.

395 Owing to the fact the C_3 fuel molecules yielded substantially higher soot masses, Fig.3d
396 showed that the proportion of the GP PAHs in propane pyrolysis was relatively low at only
397 68 % at a temperature of 1050 °C and then decreased to 40 % at 1150 °C. At a temperature
398 higher than 1150 °C, Fig.3d shows that, for propane pyrolysis, the proportion of the PP PAHs
399 on propane soot particles overtakes those in the GP PAHs and they dominated the total PAH
400 distribution up to 1250 °C. The temperature at which the PP PAHs crossed-over the GP PAHs
401 was observed earlier in propane (1150 °C) than in acetylene (1350 °C), hence, the PP PAHs
402 will only be greater than the GP PAHs in acetylene pyrolysis at temperature higher than 1350°C
403 (see Fig.3c).

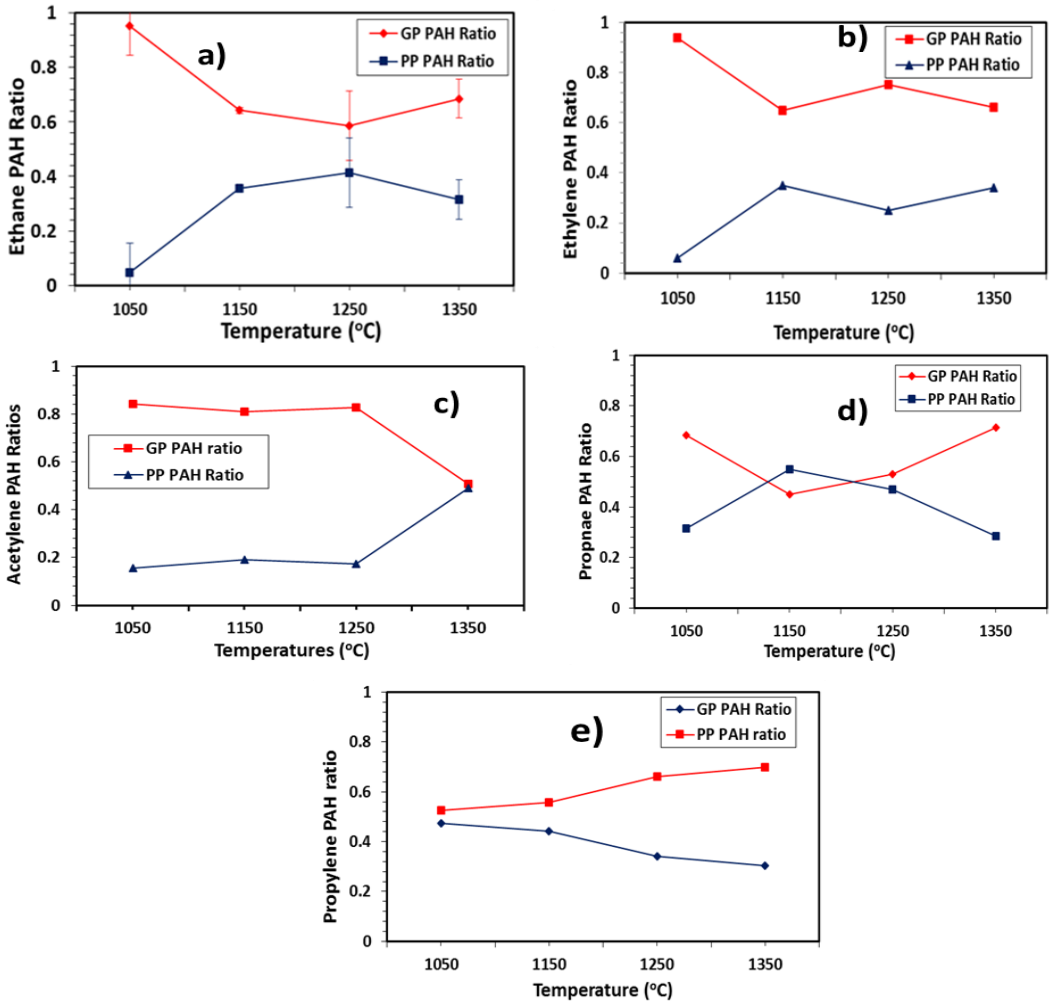

404

405 **Fig. 3: Gas phase (GP) and Particle phase (PP) PAH Ratios of C2 and C3 Fuels: a) Ethane b) Ethylene c)**
406 **Acetylene d) Propane e) Propylene ("Ratio" on the Y- axis refers to the fractional contribution of GP and**
407 **PP PAHs to the total PAHs, hence, GP ratio + PP ratio = 1)**

408 The proportions of GP and PP PAH for propylene pyrolysis are shown in Fig.3e. It can be seen
409 from the figure that the GP and PP PAHs converged initially at a temperature of < 1050 °C
410 with relative proportions of 43 % and 57 % respectively, and then diverged markedly with
411 temperature rise. The PP PAHs in propylene dominated the total PAH at higher temperatures.
412 One could hypothesise from Fig.3e that the GP PAHs probably have higher concentrations at
413 temperatures lower than 1050 °C.

414 Lighter PAHs up to and including pyrene were generally found more abundant in the gaseous
415 phase, while the heavier PAHs were found more abundantly adsorbed on the particulates.

Fig.4 summarises these observations. The 6 PAHs in Fig.4 (NPH, ACN, ACY, FLU, PHN, ATR) are categorised as the light PAHs. The four, 4ring PAHs (FLT, PYR, B[a]A, CRY) are grouped as medium PAHs, while the 6 PAHs (B(b)F, B(k)F, B(a)P, I(123cd)P, D[ah]A and B(ghi)P) are classified as the heavier PAHs [40]. Fig.4 demonstrates that as the molecular weight of the PAHs increased from naphthalene to benzo (g,h,i)perylene, the concentrations of gas phase PAHs decreased while those of the PP PAHs increased. Pyrene (a 4 ring PAH) was found in both the gas and the particulate phases in an approximately 1:1 ratio and marks the transition between the lighter PAHs mostly found in the gas phase and the heavier PAHs found mostly on the particulates.

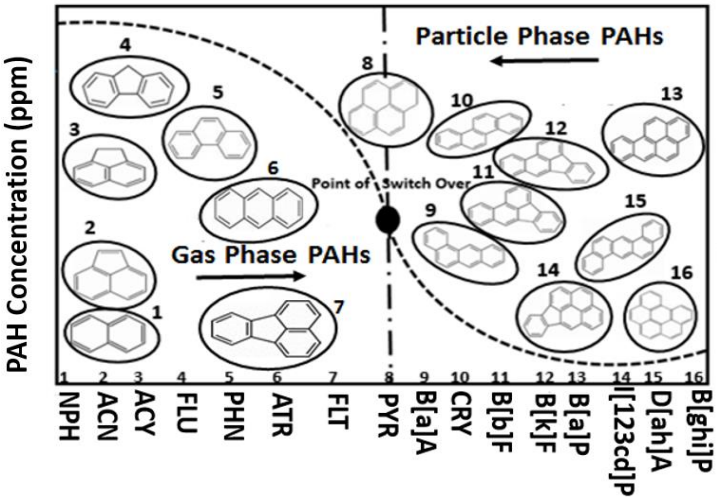

Fig.4: Summary on the increase or decrease of the particulate and gas phase PAHs as the molecular weight increases

Frenklach [20] also reported pyrene as the principal 'precursor to soot particle nucleation' which might imply that in addition to being adsorbed on the particulate, pyrene also contributes directly to the formation of larger PAHs which eventually lead to soot particle nucleation. Therefore, the transition between GP and PP PAHs occurs around 4-ring PAHs and interestingly, this observation is in agreement with that reported by Alam et al. [41] who measured atmopsheric PAHs in the city of Birmingham, UK. One limitation of the phenominological PAH distributions in Fig.4 is that it is most applicable within tempeture

range of 1150 -1250 ^{o}C of the tube reactor (and under the conditions studied), where significant proportions of both gas phase and particle phase PAHs were detected.

3.3 Growth of Individual Total PAHs

The total mass concentration of the gaseous and particulate PAHs was found by adding together the gas phase (GP) and particle phase (PP) PAH concentrations for each of the 16 individual PAH. Figure 5 shows the total concentrations of individual PAHs for all the C_2 and C_3 fuels tested. It can be observed from Fig.5a that naphthalene concentration in acetylene pyrolysis was substantially higher when compared with other fuels investigated. The abundance of naphthalene in acetylene pyrolysis agreed with the findings of other published works [17],[18] and was expected since acetylene contribute significantly to the formation of the first aromatic ring (benzene or phenyl). Formation of napthalene often follows the formation of the first aromatic ring through a number of possible pathways [1],[42], [43], [44]. One of the pathways to formation of benzene is the reaction of vinyl acetylene (C_4H_4) with acetylene (C_2H_2), with C_4H_4 formed via acetylene dimerisation [19]. The same mechanisms to benzene formation were reported in ethylene pyrolysis [23], [45].

Returning to Fig.5a, at the high temperature of 1350 ^{o}C for example, naphthalene concentrations for both ethylene and acetylene were almost the same and this agrees with the findings that the behaviour of ethylene and acetylene is identical at high temepature [32], [45]. Ethane also showed significant amount of naphthalene at 1350 ^{o}C, and likely this is because ethane could readily yield ethylene [46]. Furthermore, Fig.5 shows that various PAHs from two to four rings were obtained at mostly similar concentrations for ethane and ethylene. Turning attention to the C_3 fuel molecules now, the formation of the first aromatic ring from propane and propylene was reported to be formed via propargyl radical (C_3H_3) recombination [37],[43]. Following the formation of the first aromatic ring, the growth process to two-ring naphthalene from phenyl radicals could readily occur via the two-stage HACA mechanism

460 [23], [47]. Although it was reported that the route to naphthalene via phenyl-acetylene was
461 dominant [47], Shukla and Koshi [19] supported that the growth to naphthalene occurs from
462 phenyl radicals via the two stage HACA mechansim. Naphthalene could also be formed by the
463 self-reaction of cyclopentadenyl radicals (C_5H_5) [1], [42]. All the routes above are likely to
464 contribute to naphthalene formation with the 2-stage HACA and phenyl-acetylene pathways
465 contributing perhaps the most.

466 Once naphthalene has been formed, it could then grow further by means of the HACA
467 mechanism to the four-ring pyrene either through the five membered ring PAH acenaphthylene,
468 shown in Fig. 5b, or via the benzenoid PAH phenanthrene (Fig. 5c) [23]. Both acenaphthylene
469 and phenanthrene could be formed from naphthalene via the HACA mechanism. The
470 appreciable amounts of biphenyl compounds identified by GCMS in the products of pyrolysis
471 of most of the fuels examined suggests that phenanthrene could have grown via biphenyl
472 through the HACA mechanism. Richter et al. [5] also reported phenathrene formation via the
473 biphenyl route, but in premixed benzene flames.

474 Looking at Fig.5c more closely, it can be seen that the concentrations of phenanthrene in the
475 pyrolysis of all the fuels examined were much lower than those of pyrene (Fig 5d). This
476 comparison may imply that phenathrene was not available in sufficiently high concentrations,
477 to support pyrene formation to high concentrations. It is therefore possible that pyrene might
478 have instead grown via acenaphthylene pathway by HACA, since, the concentrations of
479 acenaphthylene in the pyrolysis of the five fuels examined was high relative to that of
480 phenanthrene. Abundance of acenaphthylene over phenantherene in ethylene and acetylene
481 pyrolyses was also reported previously by other researchers [14],[17]. An alterative,
482 contrasting, possibilty was that bezenoid-phenanthrene was observed in low concentration
483 because it was significantly depleted through readily being converted to benzenoid-pyrene.

Nevertheless, the growth of naphthalene to pyrene by the HACA mechanism, principally via acenaphthylene pathway, was found to be the dominant route [23].

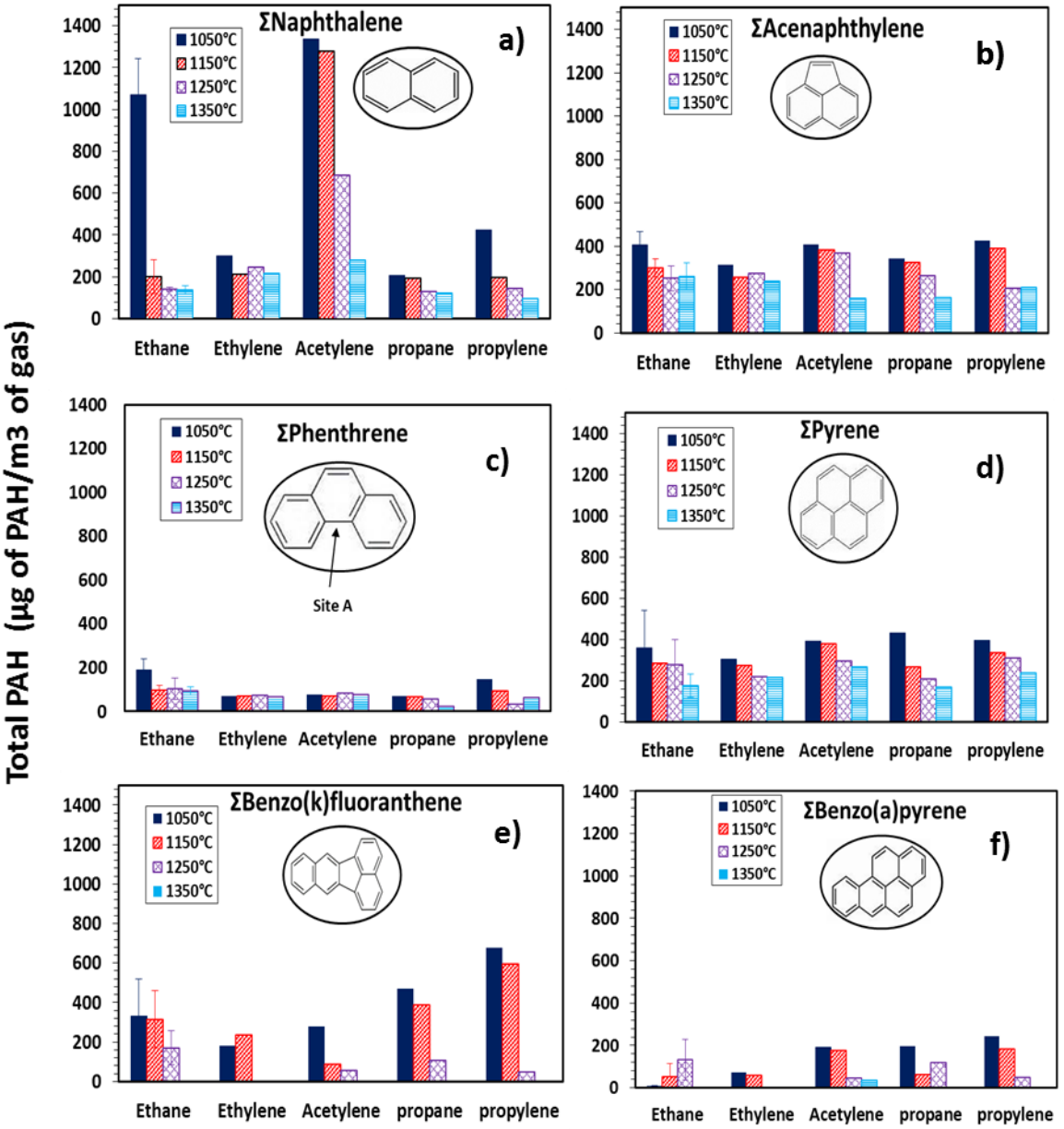

Fig.5: Distributions of total PAHs produced during the pyrolysis of C2 and C3 Fuels a) Naphthalene b) Acenaphthylene c) Phenantherene d) Pyrene e) Benzo(k)fluoranthene and f) Benzo(a)pyrene.

A possible route for the growth of acenaphthylene to fluoranthene by HACA was recently reported [19]. It can also be seen from Fig.5d that pyrene was found in approximately equal concentrations in the pyrolysis products of all the 5 fuel molecules investigated, regardless of

their degree of unsaturation. An explanation for this observation is that probably all 2 and 3 ring PAHs pass through pyrene in order to grow further to heavier PAHs.

Once pyrene or fluoranthane had been formed, further PAH growth from either of them to heavier PAHs, especially the Group B2 PAHs, could be achieved either by HACA or HAVA (hydrogen abstraction, vinyl radical addition) [19]. Other growth pathways, depending on intermediate precursors, include phenyl addition and cyclisation (PAC) as well as methyl addition and cyclisation (MAC) [48]. Further growth of the Group B2 PAHs could occur either within thesemselves or via Group D PAHs. For example, the five ring benzo(k)fluoranthene (Fig.5e) a member of Group B2 PAHs, could be formed from the three ring fluoranthene via HAVA [19]. Chrysene, also a four ring member of Group B2 PAHs, could grow from the three ring phenathrene radical by one-stage HACA. Similarly, the four ring benzo(a)anthracene could grow from the three ring anthracene and then benzo(a)anthracene could be converted to the five ring benzo(a)pyrene (Fig.5f) by means of further dehydrogenation and acetylene addition ($-H_2/+C_2H_2$) [49]. It is noteworthy mentioning that the conversion of the three ring anthracene to the four ring benzo(a)anthracene and then to the highly mutagenic five ring benzo(a)pyrene increases toxicity by 10 times at each growth stage. A two-stage HACA starting with the two ring naphthalene radical (2-naphthyl) could lead to three ring anthracene [5]. Also, isomerisation of the three ring phenanthrene to the three ring anthracene was found to be possible at temperatures > 1327^{o}C [50]. This is in agreement with the increasingly high concentrations of anthracene detected over phenanthrene at a temperature of 1350^{o}C (see Tables 5, 6 and 7) suggesting isomerisation at this higher temperature of phenanthrene to anthracene. From a view point of the stability of anthracene, it is worth mentioning here that anthracene was not detected at most of the pyrolysis temperatures for most of the fuels, since the kinked-phenanthrene was already known to be more stable than the linear-anthracene [51].

517 This notable absence of anthracene could be associated with the consistent partial sublimation
518 inherent with it [5]. The five ring mutagenic benzo(a)pyrene (Fig.5f) could be produced
519 through a number of pathways, including from the pyrene radical (2-pyrenyl) via two
520 consecutive steps of the HACA mechanism [5]. The six ring indeno(1,2,3-cd)pyrene, another
521 Group B2 toxic PAH, could be formed from a pyrene radical (4-pyrenyl) by phenyl addition to
522 4-pyrenyl. Finally, it is possible for the six ring benzo(g,h,i)perylene to be produced from the
523 four ring pyrene via several consecutive HACA steps [23].
524
525 ***3.4 Number of PAH Rings***
526 Fig.6 groups, for each fuel, the total PAH concentration according to number of rings. The
527 resulting PAH concentration for the different number of rings helps observe the growth of
528 PAHs. Fig.6 shows that regardless of the degree of unsaturation of the fuel molecules
529 investigated, the concentrations of the PAHs increased from those for two rings, peaked at three
530 rings and then tended to decrease in the case of four to five and then to six rings.

531 For exmple, in ethylene pyrolysis at temperature of 1050 ^{o}C, the concentrations of 2 ring PAHs
532 was about 200 μg/m^3, increasing morethan eightfold to >1500 μg/m^3 for the 3 ring PAHs and
533 then reduced drastically to around 500 μg/m^3 for the 4 rings, 200 μg/m^3 for the 5 rings and
534 slightly increased to about 250 μg/m^3 for the 6 ring PAHs. A similar trend was observed for all
535 the fuels and at most temperatures investigated.

536 It is evident, therefore, from Fig.6, that pyrolysis of the C_2 and C_3 fuels yielded substantially
537 higher concentrations of the 3 ring PAHs than the PAHs having 2 rings or 4 to 6 rings. The
538 three ring PAHs (which were dominated by the five membered ring and kinked PAHs such as
539 phenanthrene) were discussed ealier (in relation to Fig.5) and are believed to have major
540 impact on the growth of the 4 - 6 ring PAHs. Probably because they have more growth sites
541 *'arm chairs'* (site A in Fig.5c) at which a new ring could be completed readily through the

HACA mechanism. Furthermore, considering Fig.6a, 6b, and 6c, ethane, ethylene and acetylene had respectively significant number of two ring PAH, and the concentration of the 2 ring PAHs tended to increase with increased degree of unsaturation of the fuel.

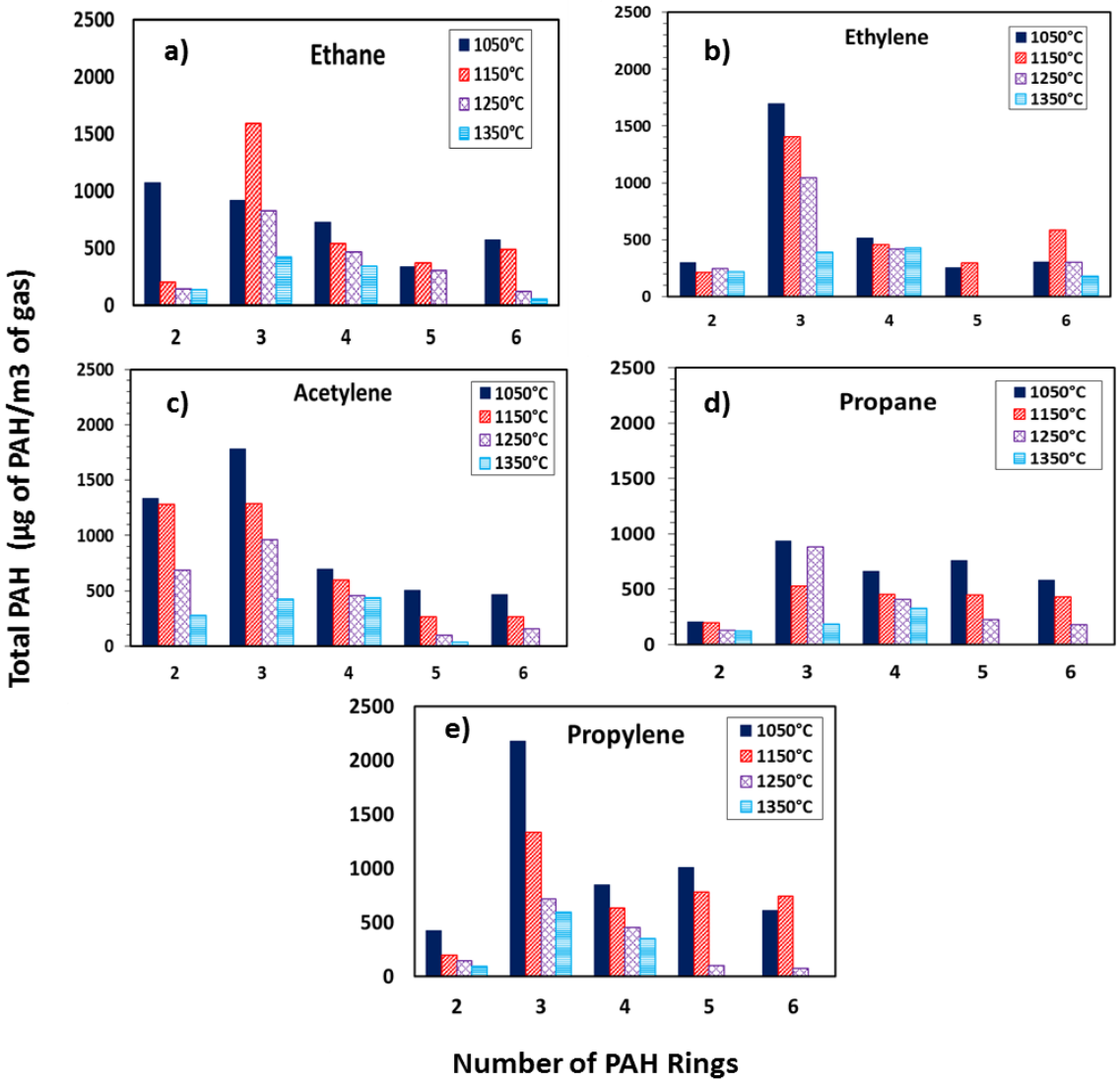

Fig. 6: Number of PAH rings of C2 and C3 Fuels: a) Ethane b) Ethylene c) Acetylene d) Propane e) Propylene

Fig.6d and 6e show that propane and propylene respectively had lower concentrations of two ring PAHs when compared with the C_2 fuels; the concentrations of the two ring PAH in the C_3 fuels also increased somewhat with increase in unsaturation of the fuel particularly at the lower temperature of 1050 ^oC. The concentrations of four ring PAHs (pyrene, fluorathene, chrysene

552 and benzo(a)anthracene) were fairly close to each other irrespective of the C_2 or C_3 fuel used.
553 Regarding the 5 and 6 ring PAHs, Fig.6 shows that the concentrations of 5 and 6 ring PAHs in
554 the C_3 fuels were somewhat higher than those in the C_2 fuels. Another observation from Fig.6
555 is that for the C_2 fuels, the concentration of the 6 ring PAHs was greater than that for the 5 ring
556 PAHs, while the converse is true for the C_3 fuels. These variations in 5 and 6 ring PAH
557 concentrations could be attributed to the way in which the 5 and 6 rings PAHs were consumed
558 for soot formation in the C_2 and C_3 fuels. In the C_2 fuels for example, the production rates of
559 the 5 ring PAHs was, possibly, faster than the consumption rates of the 6 rings to heavier PAHs
560 and eventually into, nascent soot particles. The oppsosite could possibly be the case for the C_3
561 fuels. It is noteworthy mentioning that the majority of the mutagenic group B2 PAHs are either
562 5 or 6 rings, with the exception of benzo(a)anthracene and chrysene, which are 4 ring PAHs
563 and can be seen from Fig.6 to be presenet in substantial concentrations.

564 ***3.5 Total PAH Analysis***

565 The total concentrations of gas phase and particulate PAHs are shown in Fig.7a and 7b
566 respectively. The total PAHs in Fig.7 were found by summing-up, for each fuel, the individual
567 concentrations of all the 16 PAHs that were detected at each temperature. It can be observed
568 from Fig.7a that the GP PAH concentrations per unit volume of gas of all the C_2 and C_3 fuels
569 decreased with rise in temperature from 1050 – 1350 ^{o}C. Also it can be seen from Fig.7a that
570 the triple bonded acetylene had the highest concentrations of GP PAHs in the temperature range
571 of 1050 – 1320 ^{o}C, followed by also high concentrations in the case of ethane and ethylene.
572 For instance, ethane was found to have higher concentrations of GP PAHs than ethylene at a
573 temperature of 1050 ^{o}C. Ethane shows a 25 % higher GP concentrations of PAHs than ethylene
574 at the temperature of 1050 ^{o}C, however, when the temperature was increased to 1350 ^{o}C, both
575 fuels were found to have the same concentrations of PAHs.

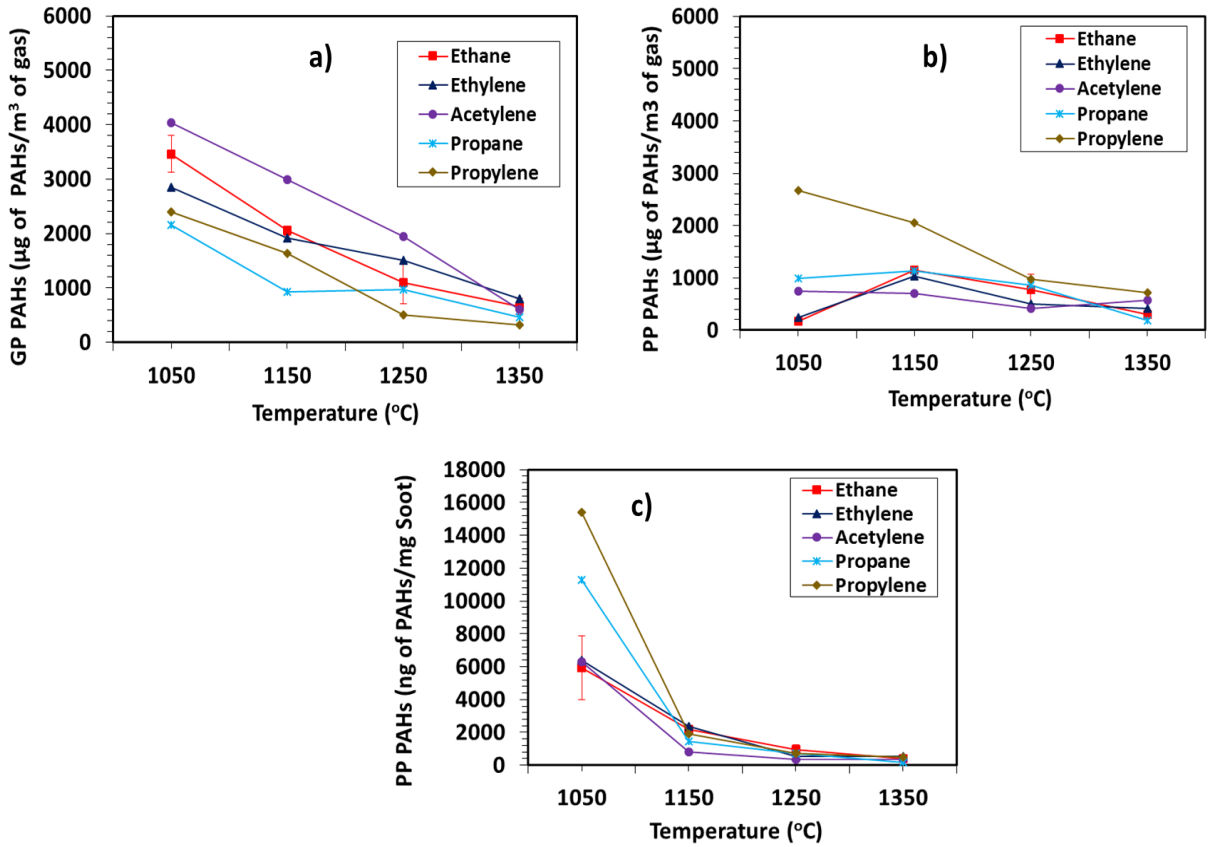

Fig. 7: Normalised Total PAH Concentrations: a) Gas Phase (µg of PAH/m^3 of gas) b) Particle Phase (µg of PAH/m^3 of gas) c) Particle Phase (ng of PAH/ mg of soot)

Fig.7a also shows that the concentrations of GP PAHs for the C_3 fuels were lower than those for the C_2 fuels at all the temperatures examined. Propylene shows higher GP PAH concentration than propane up to a temperature of 1200 °C. It would therefore appear from Fig.7a that the highly unsaturated acetylene, which is also a key growth specie in the HACA mechanism shows consistently the highest concentration of PAH at all temperatures; however, there is no such clear trend for the unsaturated C_2 and C_3 fuels (ethylene and propylene) when compared with the saturated C_2 and C_3 fuels (ethane and propane). The particle phase (PP) PAH concentrations per unit volume of gas, shown in Fig.7b, indicate that the double bonded C_3 propylene yielded the highest concentrations of PP PAHs at all temperatures compared with the other fuels investigated. The results shown in Fig.7b suggest that apart from the case of

propylene, the particle phase concentrations of PAHs per unit volume of gas were affected less by rising temperature than the GP PAHs shown in Fig.7a.

The normalised PP PAH concentrations per unit mass of soot are shown in Fig.7c. The figure shows high abundance of PAH mass concentrations at the low temperature of 1050 ^{o}C, but the concentrations decreased drastically when the tempetature rose to 1150 ^{o}C. Further decrease in the PAH mass concentrations can be seen as the temperaure was increased to 1350 ^{o}C. This observation suggest that the condensation of PP PAHs on soot particle does not only result in solvent-extractable PAH, but also that it results in incorporation of the condensed PAHs into soot particle structure.

The high mass concentration of PP PAHs at the lowest temperature of 1050 ^{o}C might additionally be related to the total surface area of the soot particles available for condensation of the PP PAHs. Measurements made with a DMS 500 particle size spectrometer in the case of ethane pyrolysis provided estimates of the total surface area at 1050 ^{o}C of 6 x 10^{6} $\mu m^{2}/cm^{3}$ of soot and at 1350 ^{o}C of 7 x10^{2} $\mu m^{2}/ cm^{3}$. The total surface area decreased substantially with temperature increase as a result of increased soot particle agglomeration which resulted in fewer, larger particles.

It is apparent from Fig. 7c that propylene yielded the highest amount of PP PAHs per unit mass of soot at 1050 ^{o}C, followed by propane. The C_2 fuels formed similar amounts of PP PAHs at 1050 ^{o}C, ethane and ethylene maintained PAH mass concentrations of similar magnitude even at higher temeparatures. It is interesting to note that this closeness in the mass concentrations of PAHs for ethane and ethylene from 1050 to 1350 ^{o}C coincides with similar soot masses for these two fuels recorded in Table 4 for the range of 1050 to 1350 ^{o}C.

Finally, returning to Fig.7a and 7b, as mentioned above, the GP PAH concentrations are seen to decrease in Fig.7a as temperature rises, while the PP PAH concentration are seen to be less sensitive to rising temperature. A posssible explanation for this is that the rate at which GP

PAHs grow and become carbonaceous soot is greater than the rate at which GP condense on particles and remain extractable by the ASE process.

3.6 Toxicity of Soot Particles

This section focuses on the Group B2 PAHs extracted from the soot particles and assesses the carcinogenicity of the particulate generated by the various fuels used. The weighted carcinogenicity of PAHs (WC-PAHs) was defined as shown equation 2, that is, as the sum of the product of each of the EPA16 priority PAH concentration (C_i) and their toxicity equivalent factor (TEF). The TEFs adopted, shown in Table 1, were those proposed by Nisbet and Lagoy [12] which are widely used by investigators to assess PAH toxicity. Since TEF is a relative factor and dimensionless and C_i has unit of concentration, WC-PAH also has units of concentration.

$$\text{WC- PAHs} = \sum_{i=1}^{16}(\text{TEF}_i * \text{Ci}) \qquad 2)$$

The weighted carcinogenicity (WC- PAHs) of the soot particles for the C_2 and C_3 fuels, on volume of gas and mass of soot bases, is shown is shown in Figs. 8a and 8b respectively. Considering Fig.8a first (gas volume basis), It is apparent that the soot particles produced from propylene pyrolysis had the highest carcinogenicity in the temperature range of 1050 – 1250 ^oC and the carcinogenicity decreased with temperature increase. For example, the weighted carcinogenicity of propylene soot particles at temperature of 1050 ^oC was 1.5 times that of propane, 3 times that acetylene and 20 times that of ethane and ethylene. This trend is due to the significantly higher amount of benzo(a)pyrene condensed on propylene soot particles. Other Group B2 PAHs that contributed to the carcinogenicity of propylene soot particles can also be seen in Tables 5, 6 and 7.

Even though propane soot particles had the second highest carcinogenicity at a temperature of 1050 ^oC, their carcinogenicity was the highest at 1250 ^oC. This result reflects high concentrations of both B(a)P and D(a,h)A on propane produced soot particles. The trends of

carcinogenicities for ethane and ethylene soot particles shown in Fig.8a were similar to their PAH concentrations shown in Fig.7b.

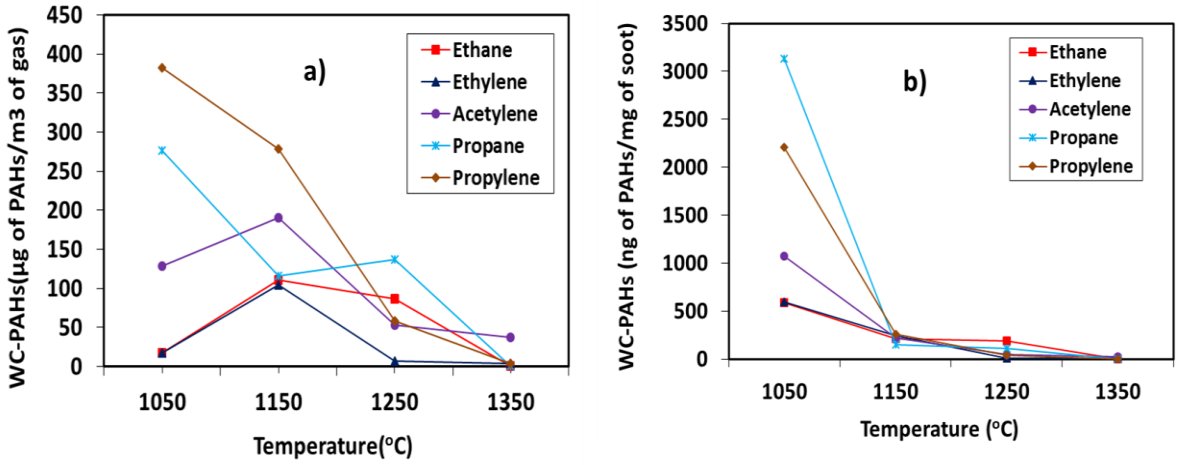

Fig. 8: Normalised Weighted Carcinogencity: a) weighted carcinogenicity of PP PAHs (µg PAH/m^3 gas) b) weighted carcinogenicity of PP PAHs (µg PAH/ g soot)

Considering now Fig.8b, which is plotted on soot mass basis, this shows that the soot particles generated from propane had the highest carcinogenicity per unit mass of soot at 1050 ^{o}C and it was found to be approximately 1.5 times that for propylene, 3 times acetylene and 5 times that of ethane and ethylene. In conclusion, while low pyrolysis temperature was associated with low abundance of soot particles, the toxicity of soot particles generated at low temperature was found to be much higher than the toxicity levels at higher temperatures. Potential implication of this observation might be that lower temperature combustion systems, for example, those designed for NOx control, may have higher overall levels of particulate WC- PAH toxicity.

4.0 Conclusions

The results of both gas-phase and particle-phase PAHs generated from the pyrolysis of ethane, ethylene, acetylene, propane and propylene were presented.

1) The degree of unsaturation of the fuels tested was observed to have a significant impact on the resulting amount of soot concentration in the effluent gas (nitrogen). The amount of soot

and the gas phase PAHs generated from the C_2 fuels were found to be increasing with increasing unsaturation in the fuels.

2) The C_3 fuels also followed a similar trend with those of the C_2 fuels, but they had greater soot yield and particle phase PAHs.

3) The particle phase PAHs included, invariably, Group B2 members, while the gas phase PAHs included members of Group D. Even though Group D PAHs are unclassifiable by the EPA in terms of carcinogenicity, however, they contribute substantially to the mechanisms of growth of the carcinogenic Group B2 PAHs.

4) There was greater abundance of PAHs (including those of Group B2) at low temperature, while higher temperatures promoted increased soot yield but lower PAH concentration in both the gas and particulate phases.

5) The total PAH concentration increased from two rings, peaked at three rings and then tended to decrease in the case of four to five and then to six rings, regardless of the degree of unsaturation of the fuel molecules investigated.

Acknowledgements

The first author wish to gratefully acknowledge the Petroleum Technology Development Fund (PTDF) for sponsoring his research studies at University College London (UCL)

References

[1] Richter H, Howard J. Formation of polycyclic aromatic hydrocarbons and their growth to soot—a review of chemical reaction pathways. vol. 26. 2000. doi:10.1016/S0360-1285(00)00009-5.

[2] Kaden DA, Hites RA, Thilly WG. Mutagenicity of Soot and Associated Polycyclic Aromatic Hydrocarbons to Salmonella typhimuriumi 1979;39:4152–60.

[3] Kim K-H, Jahan SA, Kabir E, Brown RJC. A review of airborne polycyclic aromatic hydrocarbons (PAHs) and their human health effects. Environ Int 2013;60:71–80. doi:10.1016/j.envint.2013.07.019.

[4] Gowers a M, Miller BG, Stedman JR. Estimating Local Mortality Burdens associated with Particulate Air Pollution. 2014.

[5] Richter H, Grieco WJ, Howard JB. Formation mechanism of polycyclic aromatic hydrocarbons and fullerenes in premixed benzene flames. Combust Flame 1999;119:1–22. doi:10.1016/S0010-2180(99)00032-2.

[6] Agency for Toxic Substances and Disease Registry, U.S. department of Health and Human services. Toxicological profile for Polycyclic Aromatic Hydrocarbons 1995.

[7] EFSA. Polycyclic Aromatic Hydrocarbons in Food [1] - Scientific Opinion of the Panel on Contaminants in the Food Chain 2008:1–114.

[8] Polycyclic aromatic hydrocarbons, selected non-heterocyclic (EHC 202, 1998) n.d.

[9] Levin W, Wood AW, Wislocki PG, Kapitulnik J, Yagi H, Jerina DM, et al. Carcinogenicity on Mouse Skin of Benzo-Ring Derivatives of Benzo (a) pyrene 1977;37:3356–61.

[10] Collins JF, Brown JP, Alexeeff G V, Salmon a G. Potency equivalency factors for some polycyclic aromatic hydrocarbons and polycyclic aromatic hydrocarbon derivatives. Regul Toxicol Pharmacol 1998;28:45–54. doi:10.1006/rtph.1998.1235.

[11] EPA HPA.pdf n.d.

[12] Nisbet ICT, LaGoy PK. Toxic equivalency factors (TEFs) for polycyclic aromatic hydrocarbons (PAHs). Regul Toxicol Pharmacol 1992;16:290–300. doi:10.1016/0273-2300(92)90009-X.

[13] Usepa. Provisional guidance for quantitative risk assessment of polycyclic aromatic hydrocarbons. 1993. doi:EPA/600/R-93/089.

[14] Crittenden BD, Long R. Formation of polycyclic aromatics in rich premixed acetylene and ethylene flames. Combust Flame 1973;20:359–68. doi:10.1016/0010-2180(73)90028-X.

[15] Olten N, Senkan S. Formation of polycyclic aromatic hydrocarbons in an atmospheric pressure ethylene diffusion flame. Combust Flame 1999;118:500–7. doi:10.1016/S0010-2180(99)00004-8.

[16] Smyth KC, Shaddix CR, Everest D a. Aspects of soot dynamics as revealed by measurements of broadband fluorescence and flame luminosity in flickering diffusion flames. Combust Flame 1997;111:185–207. doi:10.1016/S0010-2180(97)00017-5.

[17] Sánchez NE, Callejas A, Millera Á, Bilbao R, Alzueta MU. Polycyclic aromatic hydrocarbon (PAH) and soot formation in the pyrolysis of acetylene and ethylene: Effect of the reaction temperature. Energy and Fuels 2012;26:4823–9. doi:10.1021/ef300749q.

[18] Sánchez NE, Millera Á, Bilbao R, Alzueta MU. Polycyclic aromatic hydrocarbons (PAH), soot and light gases formed in the pyrolysis of acetylene at different temperatures: Effect of fuel concentration. J Anal Appl Pyrolysis 2013;103:126–33. doi:10.1016/j.jaap.2012.10.027.

[19] Shukla B, Koshi M. A novel route for PAH growth in HACA based mechanisms. Combust Flame 2012;159:3589–96. doi:10.1016/j.combustflame.2012.08.007.

[20] Frenklach M. Kinetic Modeling of Soot Formation with Detailed Chemistry and Physics : Laminar Premixed Flames of C 2 Hydrocarbons 2000;136:122–36.

[21] Norinaga K, Deutschmann O, Saegusa N, Hayashi J. Analysis of pyrolysis products from light hydrocarbons and kinetic modeling for growth of polycyclic aromatic hydrocarbons with detailed chemistry. J Anal Appl Pyrolysis 2009;86:148–60. doi:http://dx.doi.org/10.1016/j.jaap.2009.05.001.

[22] Lacroix R, Fournet R, Ziegler-Devin I, Marquaire PM. Kinetic modeling of surface reactions involved in CVI of pyrocarbon obtained by propane pyrolysis. Carbon N Y 2010;48:132–44. doi:10.1016/j.carbon.2009.08.041.

[23] Frenklach M, Clary DW, Gardiner WC, Stein SE. Detailed kinetic modeling of soot formation in shock-tube pyrolysis of acetylene. Symp Combust 1985;20:887–901. doi:10.1016/S0082-0784(85)80578-6.

[24] Pitz WJ, Mueller CJ. Recent progress in the development of diesel surrogate fuels. Prog Energy Combust Sci 2011;37:330–50. doi:10.1016/j.pecs.2010.06.004.

[25] Eveleigh A. The influence of fuel molecular structure on particulate emission investigated with isotope tracing 2015.

[26] Glarborg P, Østberg M, Johannessen JT, Livbjerg H, Jensen AD, Christensen TS. Formation of polycyclic aromatic hydrocarbons and soot in fuel-rich oxidation of methane in a laminar flow reactor 2004;136:91–128. doi:10.1016/j.combustflame.2003.09.011.

[27] EPA Method TO. Method TO-13A: Compendium of Methods for the Determination of Toxic Organic Compounds in Ambient Air Second Edition Compendium Method TO-13A Determination of Polycyclic Aromatic Hydrocarbons (PAHs) in Ambient Air Using Gas Chromatography / Mass Spectrom. Epa 1999.

[28] Test Methods for evaluating solid waste.pdf n.d.

[29] Richter BE, Jones B a, Ezzell JL, Porter NL. Accelerated Solvent Extraction : A Technique for Sample Preparation. Anal Chem 1996;68:1033–9. doi:10.1021/ac9508199.

[30] Oukebdane K, Portet-Koltalo F, MacHour N, Dionnet F, Desbèlne PL. Comparison of hot Soxhlet and accelerated solvent extractions with microwave and supercritical fluid extractions for the determination of polycyclic aromatic hydrocarbons and nitrated derivatives strongly adsorbed on soot collected inside a diesel particu. Talanta 2010;82:227–36. doi:10.1016/j.talanta.2010.04.027.

[31] Popp P, Keil P, Moder M. Application of accelerated solvent extraction followed by gas chromatography , high-performance liquid chromatography and gas chromatography – mass spectrometry for the determination of polycyclic aromatic hydrocarbons , chlorinated pesticides and polychl 1997;774:203–11.

[32] Ruiz MP, Callejas a., Millera a., Alzueta MU, Bilbao R. Soot formation from C2H2 and C2H4 pyrolysis at different temperatures. J Anal Appl Pyrolysis 2007;79:244–51. doi:10.1016/j.jaap.2006.10.012.

[33] Mathieu O, Frache G, Djebaïli-Chaumeix N, Paillard CE, Krier G, Muller JF, et al. Characterization of adsorbed species on soot formed behind reflected shock waves. Proc Combust Inst 2007;31 I:511–9. doi:10.1016/j.proci.2006.07.190.

[34] Markatou P, Wang H, Frenklach M. A Computacional Study of Sooting Limits in a laminar premixed flame 1993;482:467–82.

[35] Frenklach M. Reaction mechanism of soot formation in flames. Phys Chem Chem Phys 2002;4:2028–37. doi:10.1039/b110045a.

[36] Violi A, D'Anna A, D'Alessio A. Modeling of particulate formation in combustion and pyrolysis. Chem Eng Sci 1999;54:3433–42. doi:10.1016/S0009-2509(98)00460-6.

[37] Norinaga K, Deutschmann O. Detailed Kinetic Modeling of Gas-Phase Reactions in the Chemical Vapor Deposition of Carbon from Light Hydrocarbons. Ind Eng Chem Res 2007;46:3547–57. doi:10.1021/ie061207p.

[38] Miller J a., Melius CF. Kinetic and thermodynamic issues in the formation of aromatic compounds in flames of aliphatic fuels. Combust Flame 1992;91:21–39. doi:10.1016/0010-2180(92)90124-8.

[39] Wang Y, Chung SH. Effect of strain rate on sooting limits in counterflow diffusion flames of gaseous hydrocarbon fuels: Sooting temperature index and sooting sensitivity index. Combust Flame 2014;161:1224–34. doi:10.1016/j.combustflame.2013.10.031.

[40] Ballesteros R, Guillén-Flores J, Barba J. Environmental and health impact assessment from a heavy-duty diesel engine under different injection strategies fueled with a bioethanol-diesel blend. Fuel 2015;157:191–201. doi:10.1016/j.fuel.2015.04.077.

[41] Alam MS, Delgado-saborit JM, Stark C, Harrison RM. Using atmospheric measurements of PAH and quinone compounds at roadside and urban background sites to assess sources and reactivity. Atmos Environ 2013;77:24–35. doi:10.1016/j.atmosenv.2013.04.068.

[42] Frenklach M. Reaction mechanism of soot formation in flames. Phys Chem Chem Phys 2002;4:2028–37. doi:10.1039/b110045a.

[43] Miller J a., Melius CF. Kinetic and thermodynamic issues in the formation of aromatic compounds in flames of aliphatic fuels. Combust Flame 1992;91:21–39. doi:10.1016/0010-2180(92)90124-8.

[44] Norinaga K, Deutschmann O. Detailed Kinetic Modeling of Gas-Phase Reactions in the Chemical Vapor Deposition of Carbon from Light Hydrocarbons. Ind Eng Chem Res 2007;46:3547–57. doi:10.1021/ie061207p.

[45] Frenklach M, Clary DW, Gardiner WC, Stein SE. Effect of fuel structure on pathways to soot. Symp Combust 1988;21:1067–76. doi:10.1016/S0082-0784(88)80337-0.

[46] Shokrollahi Yancheshmeh MS, Seifzadeh Haghighi S, Gholipour MR, Dehghani O, Rahimpour MR, Raeissi S. Modeling of ethane pyrolysis process: A study on effects of steam and carbon dioxide on ethylene and hydrogen productions. Chem Eng J 2013;215-216:550–60. doi:10.1016/j.cej.2012.10.078.

797 [47] Bittner JD, Howard JB. Composition profiles and reaction mechanisms in a near-sooting
798 premixed benzene/oxygen/argon flame. Symp Combust 1981;18:1105–16. doi:10.1016/S0082-
799 0784(81)80115-4.

800 [48] Shukla B, Koshi M. Comparative study on the growth mechanisms of PAHs. Combust Flame
801 2011;158:369–75. doi:10.1016/j.combustflame.2010.09.012.

802 [49] Keller a., Kovacs R, Homann K-H. Large molecules, ions, radicals and small soot particles in
803 fuel-rich hydrocarbon flames. Part IV. Large polycyclic aromatic hydrocarbons and their
804 radicals in a fuel-rich benzene–oxygen flame. Phys Chem Chem Phys 2000;2:1667–75.
805 doi:10.1039/a908190i.

806 [50] Colket MB, Seery DJ. REACTION MECHANISMS F O R T O L U E N E PYROLYSIS
807 1994.

808 [51] Poater J, Visser R, Sola M, Bickelhaupt FM. Polycyclic benzenoid [why kinked arene is more
809 stable than straight]. J Org Chem 2007;72 :1134–42.

810